Friction Drag on a Cylinder Moving in a Nematic Liquid Crystal

R. W. Ruhwandl and E. M. Terentjev

Cavendish Laboratory, University of Cambridge, Madingley Road, Cambridge CB3 0HE, U. K.

Z. Naturforsch. **50 a,** 1023–1030(1995); received August 17, 1995

The flow of a liquid crystal around a body depends not only on the geometry of the body but also on the director field around it. For low-Ericksen number flows, the director distribution largely remains in its static equilibrium texture (along a uniform direction far away from the body and, for instance, perpendicular to its surface). We calculate the velocity and pressure of a cylinder in a nematic flow numerically, taking into account topological defects on the particle surface and find the drag force acting on the moving body. The drag force is, in general, non-central, *i.e.* not aligned with the direction of motion. The lift component of the drag force is a measure for the anisotropy of the system. We show that due to the realistic director texture the drag force is larger than previously thought and the anisotropy, $F_{\parallel}/F_{\perp}$, smaller and decreasing while approaching the nematic clearing point.

I. Introduction

Detailed knowledge of the viscous coefficients of a liquid crystal is vital for many applications, mainly electro-optical ones, which use the mobility and reorientation of the birefringence axis driven by external fields. (A fast response time, which is controlled by viscosity, is the goal of most such applications). It is particularly important to be able to predict the viscosity, the so-called Leslie coefficients in a nematic material, on the basis of molecular parameters like anisotropic dimensions and polarizability, and the density and temperature of the system. Such a predictive power would allow a direct synthesis of materials with precisely required properties. The initial activity in this area in the 70's [1-3] resulted in the formulation of a semi-empirical, but quite successful molecular model of Leslie coefficients by Diogo and Martins [4]. After some period of quietness, a new interest in the study of viscous properties of thermotropic nematic liquid crystals has arisen in recent years [5-9], when a consistent molecular-statistical theory has been derived and more sophisticated and accurate experiments were performed.

However, even at present our understanding of factors and effects that determine the complex viscous properties of liquid crystals is incomplete: many-body interactions in a dense molecular system, balance of attractive and steric forces, correlations and even temperature dependence away from the transition point are still unaccounted for. In this situation it is very important to provide detailed and, in particular, diverse experimental data, not always provided by standard shear viscosimeter techniques. One of the relevant alternative methods, which is also useful for determining pressure dependences and the balance between elastic and viscous forces, is the falling ball technique [2, 3]. The idea of this method goes back to the Stokes formula for the viscous drag on a sphere: $F_D = -6\pi R u \eta$, which provides the viscous coefficient η.

This problem in a liquid crystal flow has a completely different dimension, both fundamentally and practically. Any particle imposes boundary conditions on the nematic director field due to the anchoring on its surface. For topological reasons the resulting director distribution $\hat{\boldsymbol{n}}(\boldsymbol{r})$ contains defects, singular points or lines [10], see Figure 1. A fluid flow, in which the velocity field $\boldsymbol{v}(\boldsymbol{r})$ is coupled to $\hat{\boldsymbol{n}}(\boldsymbol{r})$ [11, 12], should be significantly altered in the vicinity of high director gradients. It is also known [13] that the motion of the disclination texture itself causes energy dissipation in the nematic and thus will contribute to the drag on the particle. And finally, because of the general uniaxial anisotropy in the system, the drag force becomes non-central, *i.e.* not aligned with the particle velocity $\boldsymbol{u}$:

$$F_i = M_{ik}(\hat{\boldsymbol{n}})\, u_k \;=\; M_{\perp} u_i + (M_{\parallel} - M_{\perp})(\boldsymbol{u}\cdot\hat{\boldsymbol{n}}) n_i , \quad (1)$$

Reprint requests to Dr. E. M. Terentjev.

0932-0784 / 95 / 1100-1023 $ 06.00 © – Verlag der Zeitschrift für Naturforschung, D-72072 Tübingen

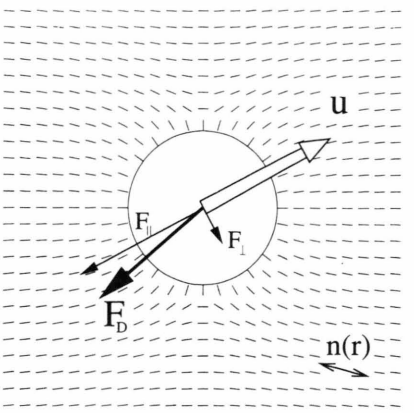

Fig. 1. The scheme of the director distribution around a cylinder satisfying the boundary condition (perpendicular to the surface) with topological defects at the poles. Moving the cylinder with velocity $\boldsymbol{u}$ causes the drag force $\mathbf{F_D}$ which is not parallel to it but includes a component $\mathbf{F}_\perp$, the lift force.

where M_{ik} is the mobility tensor with the vector indices $i, k = 1, 2, 3$, and where the last equation is valid in a uniform uniaxial sample. The component of the drag force perpendicular to the motion is called the lift force, Figure 1; it could be easily detected by the resulting displacement and it carries an additional information about the five (in the uniaxial nematic) Leslie coefficients.

The theoretical problem of a body moving through the nematic liquid crystal matrix has been addressed before. Diogo [14] has assumed that the velocity distribution $\boldsymbol{v}(\boldsymbol{r})$ around the moving sphere is the same as that for an isotropic fluid, the Stokes solution [15], and considered only the effect of specific director fields $\hat{\boldsymbol{n}}(\boldsymbol{r})$ on the drag force, in all cases assuming axial symmetry of $\hat{\boldsymbol{n}}(\boldsymbol{r})$ around $\boldsymbol{u}$. Roman and Terentjev [16] have obtained the analytical solution of the hydrodynamic problem for $\boldsymbol{v}(\boldsymbol{r})$ around the moving sphere, under the assumptions of a constant, uniform director field unaffected by the flow and of a small nematic order parameter, which allowed the series expansions in the anisotropy. Recently, in a series of papers [8, 9] Heuer, Kneppe, and Schneider developed a numerical procedure of solving the set of constitutive equations of a nematic liquid crystal flow around a particle. They, however, also ignored the nematic director non-uniformities and defects, introduced by the particle, and in all cases assumed a constant field $\hat{\boldsymbol{n}}(\boldsymbol{r}) = \hat{\boldsymbol{n}}_0$. Clearly, all these approaches have serious deficiencies, addressing just one side of the complex problem of coupled viscous and curvature elastic effects. For example, comparison of similar results for the motion with $\boldsymbol{u} \| \hat{\boldsymbol{n}}$ of Diogo [14] and of Kneppe, Schneider, and Schwesinger [9] shows a difference in the drag force of more than 13%.

In this paper we shall attempt to solve the full problem, in particular investigating the effect of high curvature gradients near the topological defects on the nematic flow. Following the example of [8, 9], we start with a simpler problem, a two dimensional analogue: the flow perpendicular to the axis of a long cylinder. As we know from classical hydrodynamics [15], this sort of two-dimensional flow is unbound and requires an outer space dimension limitation, typically chosen as an outer cylinder, concentric with the inner one. We shall assume the radial (homeotropic) boundary conditions for the director on the particle surface, which is a typical result of, for instance, treatment with a surfactant. As a consequence, a pair of two dimensional topological defects on its poles will appear (which correspond to two (–1/2) disclination lines lying along the cylinder axis). In order to model the realistic experiment in a near-infinite uniform nematic we take the director field on the outer system boundary to be constant: it is the mismatch between topological characteristics on the two boundaries that forces the singularities of $\hat{\boldsymbol{n}}(\boldsymbol{r})$ near the particle, which is a typical result of bringing a foreign body with surface anchoring into an otherwise uniform nematic liquid crystal [10].

This paper is organized as follows. In the next section we rehearse the basic ideas of fluid dynamics of nematic liquid crystals, describe the equilibrium $\hat{\boldsymbol{n}}(\boldsymbol{r})$ pattern and set the stage for a numerical solution. A very short section III describes the numerical method of artificial compressibility [17]. Section IV presents the main results of this calculation, discusses new qualitative points that arise and gives the comparison with a similar calculation of Heuer, Kneppe, and Schneider [8] (which assumed a constant director field). Finally, in Conclusions we briefly discuss the experiment and outline problems for the future.

II. Basic concepts of the theory

In this section we begin with the basic equations of nematodynamics, as they are summarized in [12]. The preferable state of a nematic liquid crystal is that all molecules are aligned parallel to one common axis. Any perturbation of this order increases the

free energy of the system, which is expressed in the distortion free energy density

$$\mathcal{F}_d = \frac{1}{2}K_1(\nabla\cdot\hat{\boldsymbol{n}})^2 + \frac{1}{2}K_2(\hat{\boldsymbol{n}}\cdot\nabla\times\hat{\boldsymbol{n}})^2 + \frac{1}{2}K_3(\hat{\boldsymbol{n}}\times\nabla\times\hat{\boldsymbol{n}})^2, \tag{2}$$

where $\hat{\boldsymbol{n}}$ is the normalized ($|\hat{\boldsymbol{n}}| = 1$) director of the molecules and K_i are the Frank constants. Since these constants in a typical thermotropic nematic are of the same order of magnitude, the one-constant approximation (with $K_1 = K_2 = K_3 = K$) is often used. This approximation, $\mathcal{F}_d = \frac{1}{2}K(\nabla\hat{\boldsymbol{n}})^2$, preserves all qualitative characteristics of the material, but is much simpler computationally. We shall adopt the one-constant approximation throughout this paper. Introducing the static molecular field $\boldsymbol{h}^o = K\nabla^2\hat{\boldsymbol{n}}$, which describes the local torque on the director, and minimising the free energy, one obtains the condition $\boldsymbol{h}^o + \lambda\hat{\boldsymbol{n}} = 0$. This means that in a static equilibrium the director is locally parallel to the molecular field [12].

If the liquid crystal is not at rest, there is an additional molecular field stemming from the viscous torques coupled to the nematic director, which must be added to the curvature-elastic one, $\boldsymbol{h}^o$, in the total equation of balance of torques:

$$h'_i = (\alpha_2 - \alpha_3)N_i + (\alpha_6 - \alpha_5)n_jA_{ij}\,, \tag{3}$$

where α_i are the Leslie coefficients. The tensor $\mathbf{A}$ represents the symmetric part of the velocity gradients [$A_{ij} = \frac{1}{2}(v_{i,j} + v_{j,i})$], and the vector $N_i = \dot{n}_i - \frac{1}{2}\left[\hat{\boldsymbol{n}}\times\operatorname{curl}\boldsymbol{v}\right]_i$ is the change of the director with respect to the background fluid. (Here and below we shall adopt the convention of summation over the repeated vector indices and the short-hand notation $B_{,j} \equiv \nabla_j B$).

For a steady state flow, the equations of motion in the low-Reynolds number limit are described by the local condition for the balance of forces on an element of volume, $\sigma_{ij,j} = 0$. The stress tensor $\boldsymbol{\sigma}$, appearing in this equilibrium condition, consists of three parts: the hydrodynamic pressure $p(\boldsymbol{r})$, a static curvature-elasticity contribution

$$\sigma^e_{ij} = -\frac{\partial\mathcal{F}_d}{\partial n_{k,j}}n_{k,i} = -Kn_{k,j}n_{k,i}\,, \tag{4}$$

where the last equation is valid in the one-constant approximation, and the viscous stress

$$\sigma'_{ij} = \alpha_1 n_i n_j n_k n_l A_{kl} + \alpha_2 n_j N_i + \alpha_3 n_i N_j + \alpha_4 A_{ij} + \alpha_5 n_j n_k A_{ik} + \alpha_6 n_i n_k A_{jk}. \tag{5}$$

Finally, since liquid crystals are usually incompressible, there is the equation of continuity $v_{i,i} = 0$ for the velocity field in a flow.

If we start with the static case ($\boldsymbol{v}$= 0) the viscous stress tensor $\boldsymbol{\sigma}'$ and the viscous part of the molecular field $\boldsymbol{h}'$ are absent. The remaining conditions for the balance of elastic forces and torques yield

$$\sigma^o_{ij,j} \equiv -p^o_{,i} + Kn^o_{k,ij}n^o_{k,j} = 0, \tag{6}$$

$$h^o_i \equiv Kn^o_{i,jj} = -\lambda n^o_i. \tag{7}$$

The static pressure due to the deformation of the director is defined by (6) and yields $p^o = \frac{1}{2}Kn_{i,j}n_{i,j}$ + const (The arbitrary constant reflects an additional external pressure and can be set equal zero without loss of generality). The static director field $\hat{\boldsymbol{n}}^o$ is given by (7), which is, of course, the usual Euler-Lagrange equation in the one-constant approximation.

The next step is to calculate the equations of motion with the fixed director field $\hat{\boldsymbol{n}}^o$, but this time with a small non-zero velocity. Pressure, velocity and director in this calculation are $p = p^o + p^1$, $\boldsymbol{v} = \boldsymbol{v}^1$ and $\hat{\boldsymbol{n}} = \hat{\boldsymbol{n}}^o$, where the superscript ^{o} relates to the static solution of (6)-(7). After some cancellations, the constitutive equations take the form

$$-p^1_{,i} + \sigma'_{ij,j}(\hat{\boldsymbol{n}}^o, \boldsymbol{v}^1) = 0, \tag{8}$$

$$v^1_{i,i} = 0. \tag{9}$$

The solution of this set, the fields p^1 and $\boldsymbol{v}^1$, are obtained as functions of the static director distribution $\hat{\boldsymbol{n}}^o$, implicitly present in $\boldsymbol{\sigma}'$, (5).

With this new solution for the velocity and pressure in a flow we are able to calculate the perturbation of the director due to the velocity field $\boldsymbol{v}^1$. The director is now given by $\hat{\boldsymbol{n}} = \hat{\boldsymbol{n}}^o + \delta\boldsymbol{n}$, where the perturbation $\delta\boldsymbol{n}$ is small and, therefore, one can keep only the leading terms in it. The equation for the molecular field yields

$$Kn^o_{i,jj} + K\delta n_{i,jj} + h'_i\big|_{\hat{n}} = 0. \tag{10}$$

The first term is zero due to the construction of the director field $\hat{\boldsymbol{n}}^o$. The viscous part of the molecular field is of the form $h' \sim \eta\nabla v^1$, where η is some average

viscosity coefficient and v^1 an average velocity. Thus (10) has the qualitative form $K\nabla^2\delta n = \eta\nabla v^1$. It is instructive to transform to the dimensionless variables in this equation, using the size of the particle as a characteristic length scale. This transformation defines the so-called Ericksen number [12] $Er = \eta v l/K$, which is a relative measure of elastic and viscous forces in the system. The order of magnitude of the correction $|\delta \boldsymbol{n}|$ due to the nematic flow is, therefore, given by

$$\nabla\delta n \sim Er \cdot v^1. \tag{11}$$

Provided the Ericksen number is small, $Er \ll 1$, the perturbation of the director field due to the slow motion of the liquid crystal is small. This perturbation will only have a small effect on the drag force and we can neglect it in the first approximation. Clearly, there is a crossover to the opposite type of behaviour, when the Ericksen number is large, $\eta v l \gg K$, and the director field is mainly determined by the flow velocity. The typical values for material parameters in this estimate are $K \sim 10^{-11}$N; $\eta \sim (5-10)\times 10^{-2}$Pa·s, so that the condition of $Er \sim 1$ amounts to $vl \sim 10^{-8}\mathrm{m}^2\,\mathrm{s}^{-1}$. For small colloid particles with sizes around $l \sim 10$ μm this corresponds to reasonably high speeds of order millimetres per second. Bigger particles require lower velocities to fall into the region of applicability of our conclusion that the static director texture around the particle is hardly disturbed by the flow. (Actually one may reasonably hope that in practice this region will be much wider, because the main effect on the drag force is coming from the near-particle volume where the velocity is lower and the director gradient higher and more strongly constrained by the surface anchoring. Experiments [3] showed that the Poiseuille-flow in a pipe even for much higher velocities appears still in the low Ericksen-number regime. The estimate above is, most likely, an overestimated upper boundary for the relevant effect).

In the effective two-dimensional problem we are considering here, Fig. 1, it is convenient to parametrize the distribution of the director by a single angle of orientation

$$n_x = \sin(\alpha),\ n_y = \cos(\alpha),\ n_z = 0,$$

so that $\hat{\boldsymbol{n}}$ is normalised for every $\alpha(\boldsymbol{r})$. It is straightforward to solve the Euler-Lagrange equation for the equilibrium distribution $\hat{\boldsymbol{n}}(\boldsymbol{r})$. Such a solution, which satisfies the boundary conditions ($\hat{\boldsymbol{n}}$ is constant and parallel to $\hat{x}$ far from the cylindrical particle and perpendicular to its surface) takes the form

$$\alpha = \arctan\left(\frac{y-R}{x}\right) + \arctan\left(\frac{y+R}{x}\right) - 2\arctan\left(\frac{y}{x}\right) - \frac{\pi}{2}. \tag{12}$$

Now we must solve the complicated anisotropic hydrodynamical problem, given by Eqs.(8)-(9), and determine the flow velocity and the pressure as functions of this director distribution.

III. Numerical Method

We used the method of Heuer, Kneppe, and Schneider [8] for the numerical calculations. Since (8) and (9) are linear, it is sufficient to consider two cases only: the flow parallel and perpendicular to the director far from the cylinder. The general direction of the flow is given by superposition of these two, as the (1) suggests.

Calculations were performed on a two-dimensional polar grid with the logarithmic radius ξ ($\xi = \ln[r/R], r = \sqrt{x^2+y^2}$, where R is the radius of the cylinder, and $\phi = \arctan[y/x]$). The choice of the logarithmic, not linear radius of polar coordinates improves the numerical efficiency by the effective coarse-graining at $r/R \gg 1$, where all gradients are expected to be small, and taking a closer look at the vicinity of the particle. We determine the velocity components $v_x(\phi,\xi), v_y(\phi,\xi)$ on the knots of the grid and the pressure points $p(\phi,\xi)$ in the centres of the meshes. The spatial derivatives were evaluated by using the next neighbours differences, e. g.

$$v_{i,\xi}(\phi,\xi) \to v_{i,\xi}(k,l) \to \frac{v_i(k,l+1)-v_i(k,l-1)}{2\Delta\xi}, \tag{13}$$

$$v_{i,\phi\phi}(\phi,\xi) \to v_{i,\phi\phi}(k,l) \to \frac{v_i(k+1,l)-2v_i(k,l)+v_i(k-1,l)}{(\Delta\phi)^2}, \tag{14}$$

$$v_{i,\phi}(k+\frac{1}{2},l+\frac{1}{2}) \to \big(v_i(k+1,l+1) - v_i(k,l+1) + v_i(k+1,l) - v_i(k,l)\big)/2\Delta\phi. \tag{15}$$

Since two dimensional flows have no solutions which would be bounded at infinity, an outer cylinder (radius R_a, in our calculations $R_a/R = 15.1$) has to be introduced with the boundary condition $\mathbf{v}(\phi, \xi_a = \ln[R_a/R]) = \mathbf{v}_o = \text{const}$.

The artificial compressibility method [17] uses the concept of time (without any real meaning) in which the system relaxes from an arbitrary distorted state to the equilibrium stationary state. This is done by an iteration in time steps, where the new velocity components are calculated by the equations of motion (8), and the new pressure by the equation of continuity (9), to which the derivative with respect to the time is added, weighted by an (arbitrary) factor c^2:

$$c^2 p_{,t} + v_{i,i} = 0. \tag{16}$$

The final "steady" state of this relaxation corresponds to the solution of $v_{i,i} = 0$, for which we are looking. Although the convergence of the iteration does not depend on the start-up state, it is preferable to use velocity and pressure as close as possible to the equilibrium state, since otherwise many time-steps are needed. We used, therefore, the analytically calculated values $\mathbf{v}(\mathbf{r})$ and $p(\mathbf{r})$ for an isotropic fluid, allowing them to evolve to a realistic solution for the liquid crystal in the process of calculation. In order to speed up the calculation the arbitrary relaxation constant c should be chosen as large as possible without causing instabilities. The choice of c depends on the size of the grid and the time-steps. Due to the symmetry of the problem, it is sufficient to perform the calculations in one quadrant of the grid only. The needed values at the boundaries and outside the grid are given by this symmetry.

The friction drag on the body was calculated by a surface integral of the stress tensor over a unit length L of the cylinder $F_i = \int \sigma_{ij} \mathrm{d}S_j$. For a flow in the $\hat{x}$-direction this integration amounts to

$$\frac{F_x}{L} = \int_0^{2\pi} \left(\cos(\phi)\sigma_{\xi\xi} - \sin(\phi)\sigma_{\phi\xi}\right) d\phi. \tag{17}$$

The necessary properties at the surface were calculated by a two step forward differentiation for the velocity derivative and a five step Lagrange extrapolation for the pressure.

IV. Results

Although it is possible to extract the analytical form of dimensional factors in expressions for $F_\parallel$ and $F_\perp$, the algebra is quite complicated and not very informative. Instead, we present the quantitative results for several characteristic sets of Leslie coefficients. We consider the experimentally known values α_i for the typical nematic material MBBA [12] and two sets produced by a theoretical model [18]. The advantage of this particular model is that it allows a consistent continuous transformation from the more conventional rod-like nematic material to a nematic of disk-like molecules. For saturated nematic order the Leslie coefficients take the form

$$\begin{aligned}
\alpha_1 &= -\frac{1}{2}\alpha_0 \left(\frac{\ell_\parallel}{\ell_\perp} - \frac{\ell_\perp}{\ell_\parallel}\right)^2; \\
\alpha_2 &= \frac{1}{2}\alpha_0 \left(1 - \left[\frac{\ell_\parallel}{\ell_\perp}\right]^2\right); \\
\alpha_3 &= \frac{1}{2}\alpha_0 \left(1 - \left[\frac{\ell_\perp}{\ell_\parallel}\right]^2\right)^2; \\
\alpha_4 &= \alpha_4;\ \alpha_5 = -\alpha_2;\ \alpha_6 = \alpha_3,
\end{aligned} \tag{18}$$

where $\ell_\parallel$ and $\ell_\perp$ are the molecular dimensions along and perpendicular to its axis of symmetry and α_0 is the dimensional factor, typically of order $\sim 10^{-1}$ Pa·s. We chose for α_4 the same value as for MBBA and determined α_0 by comparing α_2, the largest anisotropic viscosity of MBBA, with the model [18]. A rod-like mesogenic molecule corresponds to $\ell_\parallel/\ell_\perp \sim 5/2$, while for the discotic material we take $\ell_\parallel/\ell_\perp = 2/5$. It is particularly interesting to examine the friction drag in the discotic nematic, because it is known [19] that these materials have qualitatively different rheological properties due to the different relation between the α_i's.

An important characteristic of the motion is the ratio of the two principal values of the drag force, $F_\perp/F_\parallel$, which informs us of the relative strength of the lift force. It is interesting that this ratio clearly decreases in all realistic cases, in comparison with the similar result for the unphysical uniform director field [8]. For instance, taking the Leslie coefficients for MBBA, we obtain

$$\frac{F_\perp}{F_\parallel}\Big|_{\mathrm{MBBA}} = 1.75 \tag{19}$$

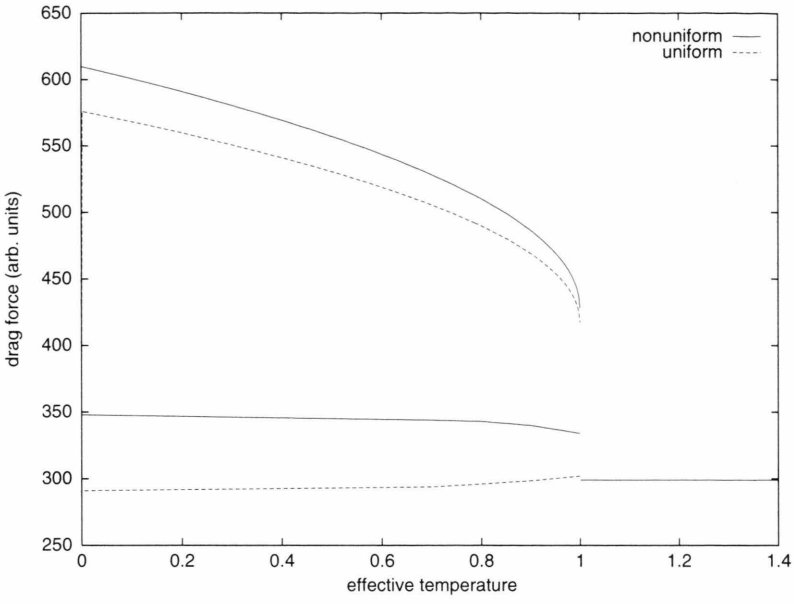

Fig. 2. Dependence of the force on the effective temperature T/T_c. For temperatures greater than 1, the force is calculated as for an isotropic liquid ($S = 0$). The upper pair shows the perpendicular case ($\hat{\boldsymbol{n}}(\infty) \parallel y$), the lower the parallel case ($\hat{\boldsymbol{n}}(\infty) \parallel x$), the solid lines represent the case of the nonuniform, the dashed lines the one of the uniform director.

instead of 2.02 for a fixed uniform director. Note that for symmetry reasons there is no lift force in the particular cases, expressed by the $F_\perp$ and $F_\parallel$ values (*i. e.* when the particle motion is parallel or perpendicular to the undistorted director). The lift force becomes maximal at a certain oblique angle between $\boldsymbol{u}$ and $\hat{\boldsymbol{n}}$ (see Fig. 1): for MBBA the maximal angle between $\boldsymbol{u}$ and $\mathbf{F}_D$ is $\theta_{\max} = 15.2°$ for an angle $\gamma = 37.1°$ between velocity and director. This should be compared with the similar results for a fixed uniform director [8] $\theta_{\max} = 19.2°$ for $\gamma = 35.4°$.

Similar results for the theoretical sets of Leslie coefficients [18] for rod-like ($\ell_\parallel/\ell_\perp = 5/2$) and for disk-like ($\ell_\parallel/\ell_\perp = 2/5$) nematic liquid crystals are:

$$\frac{F_\perp}{F_\parallel}|_{\text{rod}} = 1.48,\ \theta_{\max} = 11.6° \text{ for } \gamma = 39.5°, \quad (20)$$

$$\frac{F_\perp}{F_\parallel}|_{\text{disk}} = 0.4,\quad \theta_{\max} = 25.7° \text{ for } \gamma = 57.7°. \quad (21)$$

We can conclude that in all situations (for realistic MBBA and for two extreme model cases) a lift force perpendicular to the velocity of the flow exists, since the ratio of the drag forces $F_\perp/F_\parallel$ is not unity. For the rod-like molecule this ratio is larger than unity, which results in a maximal lift force for an angle $\gamma < 45°$, whereas for the disk-like case $F_\perp/F_\parallel < 1$, and therefore $\gamma > 45°$. The fact that the drag force $F_\perp$ is smaller than $F_\parallel$ for the discotic nematic is reasonable: the director represents here the shorter axis of the molecules. Therefore, a flow parallel to the director is a flow perpendicular to the longer axis which has clearly a larger resistance than a flow perpendicular to the shorter axis.

Another important aspect is the comparison with the case of the uniformly constrained director [8]. For the rod-like nematic the ratio $F_\perp/F_\parallel > 1$ is decreased, mainly due to the large increase in $F_\parallel$ (see Figure 2). The reason for such an increase is that the director is perpendicular to the flow and has a large gradient in the region of the topmost point of the cylinder (12 o'clock in Figure 1) with the effect that the fluid is slowed down. For the uniform director this was the point with the largest velocity, which is now decreased drastically (see Figure 3). The liquid crystal passes the cylinder further away in average. The same applies to the lowest point (6 o'clock).

For the perpendicular case $F_\perp$ it is the other way round: the significant change in the director at the horizontal ends (3 and 9 o'clock) increases the resistance to the flow, but in the regions of the lower fluid velocity. Therefore the drag effect in this case is much smaller than for $F_\parallel$.

The influence of the non-uniform director-field around the cylinder cannot simply be covered by choosing a larger effective radius and using a uniform field. The situation is more complicated and there are at least two different values for the effective radii for

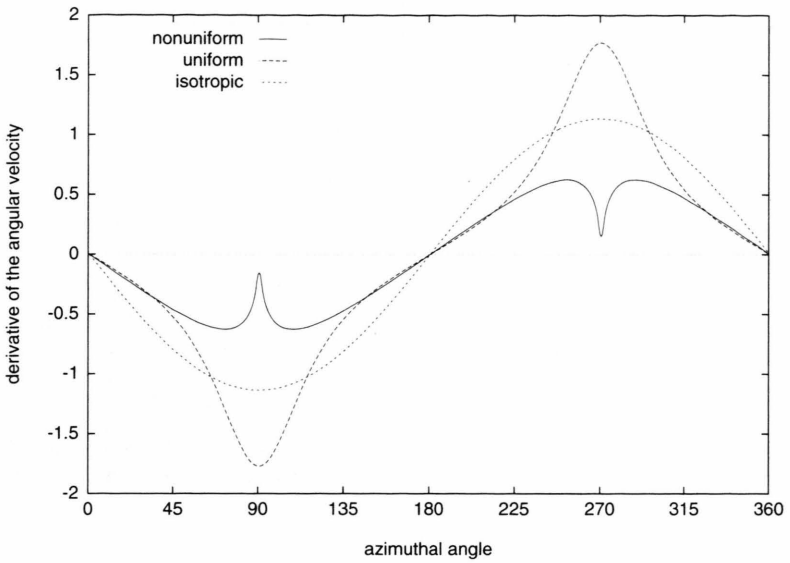

Fig. 3. Radial derivative of the angular velocity $v_{\phi,\xi}$ at the surface of the cylinder over the azimuthal angle ϕ. The three graphs show the values for the nonuniform director, the uniform director (where the director is parallel to the flow) and for an isotropic fluid. (The singularities of the director field are at $\phi = 90°$ and $\phi = 270°$).

the two orientations. The best approximation would probably be to use an effective elliptic cross-section, but that is not very useful for the calculations.

The temperature behaviour of the drag force is also of great interest. The viscous coefficients $\alpha_1, \alpha_2, \alpha_3, \alpha_5$, and α_6 can be assumed to depend linearly on the order parameter S close to the critical temperature, whereas α_4 can be regarded as constant. The order parameter S itself for liquid crystals can be qualitatively, but quite adequately modelled by the temperature dependence $S = 0.4 + 0.6 * \sqrt{|\, T/T_c - 1 \,|}$. We scale the viscous coefficients with the (small) order parameter (see theoretical models [5, 18]):

$$\alpha_1 \to \alpha_1 * S;\ \alpha_2 \to \alpha_2 * S;\ \alpha_3 \to \alpha_3 * S;$$
$$\alpha_4 \to \alpha_4; \qquad \alpha_5 \to \alpha_5 * S;\ \alpha_6 \to \alpha_6 * S. \tag{22}$$

The calculations show (Fig. 2) that the parallel and the perpendicular drag forces are larger for lower temperatures for the nonuniform field. This prediction with respect to $F_{||}$ is clearly different from the one obtained for the uniform field. The ratio of the two forces is increasing in both cases, which is expected because lowering the temperature means increasing the order of the molecules in the liquid crystal and therefore increasing its anisotropy.

V. Conclusion

The drag force acting on a cylinder moving in a liquid crystal was examined for a realistic director field. It was chosen to fulfil the boundary conditions at the cylinder (director perpendicular on the surface) and was obtained by solving the static problem. It contains topological defects on the surface of the body and was assumed to be fixed (independent of the velocity), which is a valid assumption in the limit of small Reynolds and Ericksen numbers.

Due to the linearity of the equations of motion, it is sufficient to calculate only two situations: The flow perpendicular and parallel to the director (at infinity). Out of combinations of these two, every angle between director and velocity can be calculated: $F_i = M_{ik}(\hat{\boldsymbol{n}})v_k$. The mobility tensor $\mathbf{M}$ is determined by the director configuration.

As expected, the drag force was larger for the nonuniform field than for the uniform one in every situation, but it is not possible to approximate this increase by simply assuming a (larger) effective radius of the cylinder. The change in the force for the two orientations is too different.

This is also reflected in the ratio of the drag forces (perpendicular/parallel to the velocity), which is significantly smaller for the nonuniform field that includes singularities of $\hat{\boldsymbol{n}}(\boldsymbol{r})$. This ratio is a measure of the lift force (the contribution of the friction

perpendicular to the velocity of the flow, due to the anisotropy of liquid crystals). The drag force would act with an angle with the flow velocity up to 15.8° (19.2° for the uniform field). It is interesting that the drag force anisotropy is reversed for the typical set of Leslie coefficients for a discotic nematic liquid crystal.

The dependence of the drag force on the temperature was also examined. It is larger for lower temperatures due to the higher order in the liquid crystal and higher viscous anisotropy. Not only the forces themselves, but also their ratio increases, which enlarges, as expected, the anisotropic behaviour.

The numerical calculations were all based on the so-called artificial compressibility method. It makes use of an (artificial) time in which the discretized system relaxes from a distorted start-up configuration to its equilibrium state. The advantages of this method are a) the possibility of deriving the governing equations directly from the basic equations of motion and b) that the numerical procedure is a linear iteration. There are disadvantages such as the long time it takes to reach convergence (especially for the large grids which were needed for the calculations with the nonuniform field) and the impossibility to obtain an analytic value for the accuracy of the calculations (due to the extremely long equations used in the program). It is, however, a very direct way to obtain the hydrodynamic properties in this complex area of fluid dynamics.

To compare the results with the actual behaviour of bodies moving in liquid crystals, it would be necessary to do some experiments. They should be done with long stiff threads (for example needles). There are two principal methods: Either moving the body with an external force (electric or magnetic field, gravitation) and measuring the velocity and the angle between the movement and the force, or controlling the direction of the movement and measuring the velocity for two (perpendicular) directions. In both cases it is necessary to do the measurements for different lengths of the bodies to estimate the effect due to the influence of the cylinder ends.

Acknowledgements

We acknowledge useful and stimulating discussions with M. Warner, J. Melrose and F. M. Leslie. We appreciate the financial support from the Unilever PLC (EMT) and the DAAD (German Academic Exchange Service - RWR).

[1] C. Gähwiller, Mol. Cryst. Liq. Cryst. **20**, 301 (1973); J. Prost and H. Gasparoux, J. Physique **32**, 953 (1971); H. Kneppe and F. Schneider, Mol. Cryst. Liq. Cryst. **65**, 23 (1981); B. C. Benicewicz, J. F. Johnson, and M. T. Shaw, Mol. Cryst. Liq. Cryst. **65**, 111 (1981).

[2] E. Kuss, Mol. Cryst. Liq. Cryst. **47**, 71 (1978).

[3] A. E. White, P. E. Cladis, and S. Torza, Mol. Cryst. Liq. Cryst. **43**, 13 (1977).

[4] A. C. Diogo and A. F. Martins, J. Physique **43**, 779 (1982).

[5] M. A. Osipov and E. M. Terentjev, Z. Naturforsch. **44a**, 785 (1989).

[6] S.-T. Wu and C.-S. Wu, Phys. Rev. **A42**, 2219 (1990).

[7] K. Devanand, J. Chem. Phys. **98**, 6567 (1993); G. Christoph, W. Stille, and G. Strobl, Intl. J. Phys. Chem. **97**, 1315 (1993); H. H. B. Meng, L. R. Dalton and S.-T. Wu, Mol. Cryst. Liq. Cryst. **250**, 303 (1994).

[8] H. Heuer, H. Kneppe, and F. Schneider, Mol. Cryst. Liq. Cryst. **200**, 51 (1991).

[9] H. Kneppe, F. Schneider, B. Schwesinger, Mol. Cryst. Liq. Cryst. **205**, 9 (1991) .

[10] E. M. Terentjev, Phys. Rev. E **51**, 1330 (1995).

[11] F. M. Leslie, Arch. Rat. Mech. Anal. **28**, 265 (1968).

[12] P. G. de Gennes and J. Prost, Physics of Liquid Crystals, 2nd edition, Clarendon, Oxford 1993.

[13] H. Imura and K. Okano, Phys. Lett. **42A**, 403 (1973).

[14] A.C. Diogo, Mol. Cryst. Liq. Cryst. **100**, 153 (1983).

[15] J. Happel and H. Brenner, Low Reynolds number hydrodynamics, 2nd edition, Martinus Nijhoff, The Hague 1983.

[16] V. G. Roman and E. M. Terentjev, Colloid J. USSR **51**, 435 (1989).

[17] R. Peyret and T. D. Taylor, Computational Methods for Fluid Flow, New York 1983.

[18] H. Ehrentraut and S. Hess, Phys. Rev. E **31**, 2203 (1995)

[19] T. Carlsson, J. Physique **44**, 909 (1983); J. T. Mang, S. Kumar, and B. Hammouda, Europhys. Lett. **28**, 489 (1994).